Turkish Journal of Physics

http://journals.tubitak.gov.tr/physics/

Research Article

Turk J Phys
(2017) 41: 410 – 417

doi:10.3906/fiz-1704-2

# Investigation of a novel temperature-sensing mechanism based on strain-induced optical path-length difference in a multicore optical fiber

**Belkıs GÖKBULUT, Sema GÜVENÇ, Mehmet Naci İNCİ***
Department of Physics, Boğaziçi University, Bebek, İstanbul, Turkey

**Received:** 03.04.2017 • **Accepted/Published Online:** 02.08.2017 • **Final Version:** 10.11.2017

**Abstract:** A four-core optical fiber is employed to investigate a novel temperature-sensing mechanism, which is based on the strain-induced optical path-length difference between the fiber core pairs. A short segment of a four-core fiber is wound around a solid stainless steel cylinder to form a tight circular loop, which is exposed to temperatures of up to 100 $^\circ$C. Temperature-induced radial expansion of the stainless steel cylinder causes a shear strain in the fiber and introduces an optical path-length difference between the fiber core pairs. This results in a total phase shift of about 20.40 $\pm$ 0.29 rad in the interference pattern of the four-core fiber, which is monitored by a CMOS camera. The temperature-induced phase and strain sensitivities are measured to be 3.74 rad/m$^\circ$C and 0.18 $\mu\varepsilon/^\circ$C, respectively.

**Key words:** Fiber optics, sensors, interferometry, temperature, phase shift

## 1. Introduction

Measurement of specific conventional physical parameters such as temperature, strain, pressure, bending, vibration, humidity, or magnetic field in an ingenious scientific way has always been the main motivation behind the research in the field of sensing technology. Interferometric fiber optic sensors have taken a particularly significant role in this area by introducing cost-effective optical devices with high sensitivity, small size, light weight, and sustainability against high temperatures [1–6].

Several former studies have made use of multicore and photonic crystal fibers in the measurement of temperature and strain sensing. For example, Antonio-Lopez et al. [7] sandwiched a segment of 2–3 cm of seven-core fiber between two single mode fibers by splicing them to each other, thus constructing a Fabry–Perot type interferometer to measure temperatures of up to 1000 $^\circ$C with an accuracy of 29 pm/$^\circ$C. In another study, a piece of hollow-core fiber was connected at both ends to standard single-mode fiber to construct a modal interferometer for both temperature and strain measurements. The resolutions were reported to be 1.4 $\mu\varepsilon$ and 0.2 $^\circ$C for strain and temperature, respectively [8]. Four-core optical fibers were used previously in two-axis bend measurement [3] and three-dimensional optical profilometry [9]. Recently, Guvenc et al. successfully used the same type of fiber to demonstrate that a four-core optical fiber can be used as a calorimetric gauge in heat transfer measurements [10]. The sensitivity of the device was given to be 7.37 $\times$ $10^{-6}$ K$^{-1}$.

In this paper, an interferometric fiber optic temperature-sensing mechanism based on shear strain in a four-core optical fiber is demonstrated. A four-core optical fiber allows guiding four mutually coherent light beams within a single cladding of 125 $\mu$m in diameter and is capable of producing an interference pattern of

*Correspondence: naci.inci@boun.edu.tr

square-like strips at the far field [3]. One may assume that each fiber core corresponds to an arm of a Michelson or Mach–Zhender interferometer to form an interferogram. A few centimeters of the four-core fiber is wound around a solid stainless steel cylinder to obtain a tight circular loop, which is exposed to temperature rise. The temperature-induced radial expansion of the stainless steel cylinder introduces a shear strain in the fiber loop, which causes an optical path-length difference between the four guiding beams in the inner and outer core pairs. This results in a phase shift in the interference pattern of the four-core fiber, which is monitored by a CMOS camera, giving a monotonic relationship between the temperature and phase of the guiding laser light. The method also allows determining the value of the shear strain with good precision.

A straight piece of a four-core optical fiber is totally immune to any temperature changes under normal circumstances since there are no cavities to cause any optical imbalance in the addressing fiber, provided that the fiber is much longer than the coherence length of the laser source. However, since the four-core optical fiber is quite sensitive to any bending due to the strain effects [3], such a mechanism is utilized to build a strain-based temperature-sensing mechanism, which is considered to be the unique feature of this work. In addition to the temperature measurements using the thermal expansion of a known cylindrical material, one may measure the thermal expansion of unknown materials with the proposed experimental arrangement since the working mechanism allows to relate the phase shift to the temperature change, strain, and thermal expansion of the material in concern.

The layout of the paper includes the strain-induced phase shift related to the optical path-length difference, which is followed by the experimental results, discussions, and a conclusion.

## 2. Principle of the method

A four-core optical fiber is used to obtain the interference of four coherent light beams. A schematic illustration of a four-core optical fiber and its corresponding interference fringe pattern are shown in Figures 1a and 1b. There are six couplings of the fiber cores, which introduce four different interferograms. A vertical interferogram is formed by pairings of the horizontal cores, a horizontal interferogram is generated by couplings of the vertical cores, and the pairings of the diagonal cores produce two opposite diagonal interferograms. The superposition of these enables an interferometric fringe pattern, which is shown in Figure 1b.

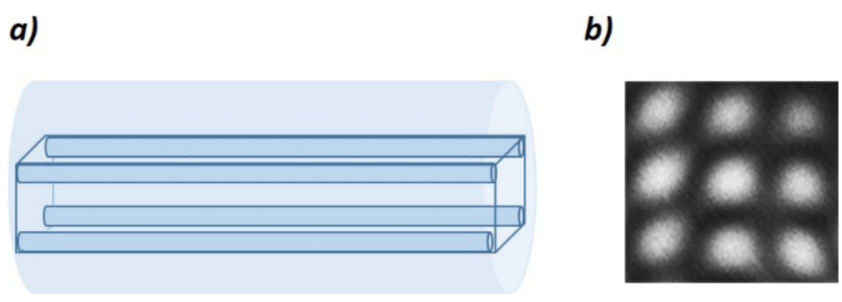


**Figure 1.** (a) Schematic representation of a four-core optical fiber and (b) its real interferometric fringe pattern.

The intensity distribution of the fringe pattern from a four-core optical fiber is given by [9]:

$$I(x,y) = 2I_O \begin{bmatrix} 2 + 2\cos\left(2\pi\frac{\delta}{\lambda f}\left(x\cos\theta - z(x,y)\sin\theta\right)\right) \\ +2\cos\left(2\pi\frac{\delta}{\lambda f}\left(y\cos\theta - z(x,y)\sin\theta\right)\right) \\ +\cos\left(2\pi\frac{\delta}{\lambda f}\left((x+y)\cos\theta - z(x,y)\sin\theta\right)\right) \\ +\cos\left(2\pi\frac{\delta}{\lambda f}\left((x-y)\cos\theta - z(x,y)\sin\theta\right)\right) \end{bmatrix} \tag{1}$$

where $\lambda$ is the wavelength of the light beam, $I_0$ is the intensity, $f$ is the focal length of the lens, $\theta$ is the illumination angle, $\delta$ is the separation distance between horizontal and vertical cores, and $x$, $y$, and $z$ are the coordinates of the interferogram. However, in this work, the fringe pattern on the CMOS camera and the cores are illuminated by a laser beam at a zero-degree angle. Therefore, when $z = 0$ and $\theta = 0$, the intensity equation becomes the following:

$$I(x,y) = 2I_O \begin{bmatrix} 2 + 2\cos\left(2\pi\frac{\delta}{\lambda f}(x)\right) \\ +2\cos\left(2\pi\frac{\delta}{\lambda f}(y)\right) \\ +\cos\left(2\pi\frac{\delta}{\lambda f}((x+y))\right) \\ \cos\left(2\pi\frac{\delta}{\lambda f}((x-y))\right) \end{bmatrix} \tag{2}$$

As the temperature is varied in the vicinity of the four-core fiber shown in Figure 1a, no path difference is expected to occur between the guiding four cores to cause any fringe shifts since all the cores experience the same thermal expansion and the same thermal optical effects. However, if one makes the same fiber as a tight circular loop around a cylindrical object and lets the cylinder radially expand, as seen in Figure 2, then $\Delta l$ path-length difference occurs between the inner and outer core-pairs since the outer core-pairs would be elongated more due to the presence of a shear strain. Exposing the cylindrical object to a temperature rise for a radial expansion is the principal idea behind our novel strain-based fiber optic temperature sensing method.

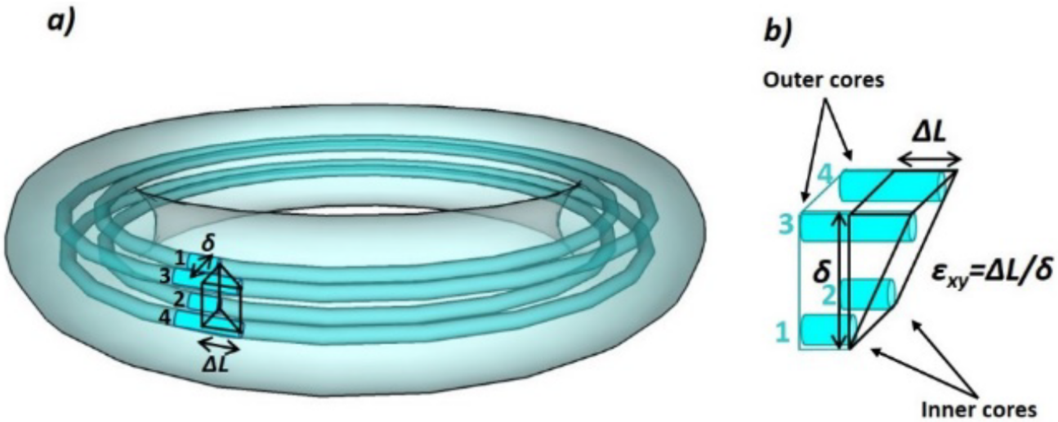


**Figure 2.** (a) Schematic representation of the strain-induced path-length difference between inner and outer core lengths and (b) enlarged picture of the path length difference.

One can express the phase of the guiding light in the fiber cores as:

$$\phi = \frac{2\pi nl}{\lambda} \tag{3}$$

where $n$ is the refractive index and $l$ is the sensitive part of the fiber length. The strain ($\varepsilon$)-dependent phase difference corresponding to the changes in the refractive index and the length is given by:

$$\frac{\partial\phi}{\partial\varepsilon} = \frac{2\pi}{\lambda}\left(n\frac{\partial l}{\partial\varepsilon} + l\frac{\partial n}{\partial\varepsilon}\right) \tag{4}$$

The strain-induced phase difference between the inner and outer two cores is given by [11]:

$$\Delta\phi = \frac{2\pi}{\lambda}\Delta l\left(n - Kn^3\right) \tag{5}$$

where $\lambda$ is the wavelength of the guiding beam and $\Delta l$ is the length difference of one inner and one outer core after strain-induced stretching, for example 1-3, 2-4, 1-4, or 2-3. For fused silica fiber, n = 1.46 and K = 0.103 [12] are taken. Since the phase change is experimentally measured by a CMOS camera, $\Delta l$ is easily calculated via Eq. (5), which allows us to determine shear strains $\varepsilon_{xx}=\frac{\Delta l}{l}$ and $\varepsilon_{xy}=\frac{\Delta l}{\delta}$ , where $l$ is the length of the fiber loop and $\delta$ is the separation between the two cores, as shown in Figure 2.

## 3. Experimental setup

A schematic representation of the experimental setup is given in Figure 3. Linearly polarized light from a He-Ne laser with the emission wavelength of 632.8 nm is coupled into a four-core optical fiber of about 45 cm in length using a 21× microscope objective lens to produce the interference fringe pattern shown in Figure 1b. A polarizer was located at the end of the fiber, before the screen, to obtain a fully polarized light in order to improve the fringe quality. In this experiment, a Glen type polarizer was used to work with only p-polarized light. Since the four cores are embedded in a single cladding with a bare fiber diameter of 125 $\mu$m, four cores act as mutually coherent sources to produce an interference pattern. Each core has a diameter of 10.6 $\mu$m and the distance between adjacent cores is 40.6 $\mu$m. The details of the four-core fiber can be found elsewhere [13].

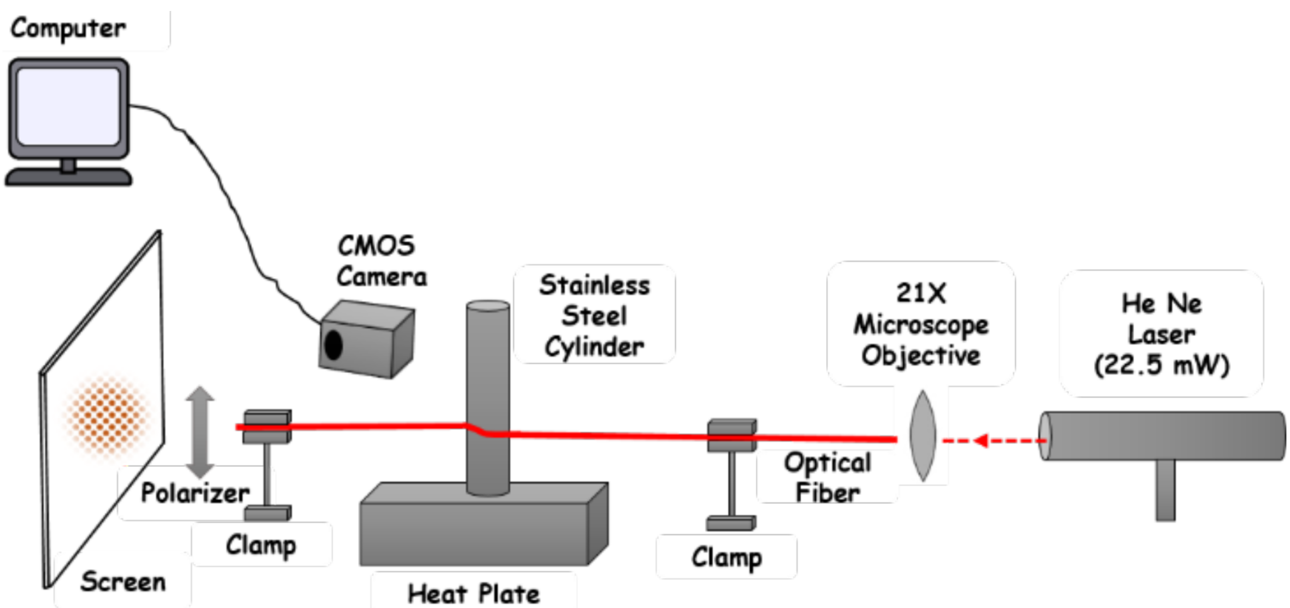


**Figure 3.** Schematic representation of the experimental setup.

After a desired fringe pattern is obtained on the screen and monitored by a CMOS camera, a fiber length of about 12 cm is wound around a stainless steel cylindrical rod with a diameter of 3.77 cm. The fiber ends are clamped to obtain a very tight circular loop for a shear strain in the four-core fiber to be effective as the metal rod thermally expands. The steel rod is placed on a heat plate, which is used to control the temperature and to provide thermal expansion of the rod. The temperatures of the fiber loop and the heat plate are assumed to be the same since the fiber loop was placed very close to the touching end of the rod with the heat plate.

## 4. Results and discussion

The heat plate is turned on to run from room temperature up to 100 °C. It is observed that the phase does not show any changes until the heater's temperature reaches about 40 °C, which means that the thermal expansion of the steel rod is not sufficiently large enough to initiate a desired strain for a phase shift between the fiber cores since the circular fiber loop around the metal rod is not amply tight. Therefore, the temperature interval from 50 °C to 92 °C is studied in our experiments to observe a clear phase change. The diameter of the stainless steel rod is measured by Vernier calipers at 50 °C and at 92 °C. The amount of the radial expansion of the steel rod causing a shear strain to the fiber ring is measured to be about 0.02 mm. Due to the geometry of the fiber ring, the outer core pairs are more stretched than the inner ones, which leads to an optical path-length difference between the wave-guiding cores. This results in a phase variation, which is monitored and stored by a CMOS camera. A MATLAB code is used to analyze the stored interferogram frames during the phase change. When the phase shift occurs, the intensity distribution of the selected part of the fringe pattern varies. Since the observed phase shift is two-dimensional, our vertical and horizontal software reference lines, which are placed on the pictures in the MATLAB domain, allow us to analyze the intensity distributions on these directions. After horizontal and vertical phase shifts are calculated, the total phase change is determined using the Pythagorean theorem.

Although the phase shift itself is periodic in nature, such a shift is observed as a continuous flow away on the screen of the fast CMOS camera and then the data are stored. Therefore, the dynamic range of the sensor is not limited by the period. Figure 4 shows the interference patterns for two different temperatures (50 °C and 92 °C). Since the pattern repeats itself after every $2\pi$ phase shift, the shift looks very slight due to a total phase shift of about 20.40 rad.

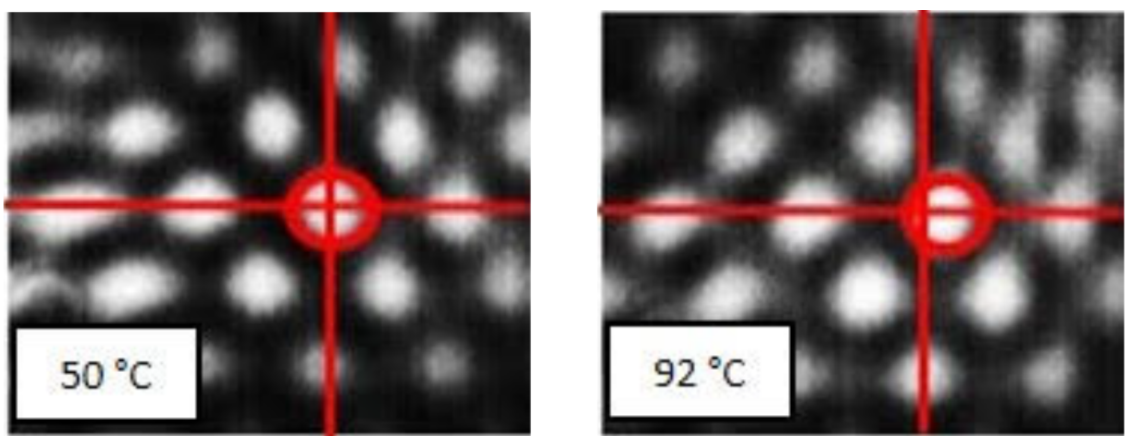


**Figure 4.** Interference patterns for two different temperatures (50 °C and 92 °C).

Figure 5 shows temperature versus phase shifts due to the path differences between various fiber core pairs, i.e. cores 1-3 plus 2-4 and cores 1-4 plus 2-3, together with the total phase shift versus temperature. As seen from the fit in the graph, a monotonic linear relationship between phase and temperature is obtained. If one assumes that $e_1$ and $e_2$ are the phase shift principle axes (see inset of Figure 5), the temperature-induced phase shift in the $e_1$ direction would be due to cores 1-3 plus 2-4 and the phase shift in the $e_2$ direction is due to cores 1-4 plus 2-3. In Figure 5, for the temperature range from 50 °C to 92 °C, a net phase shift of 18.8 rad is measured in the $e_1$ direction and 8.01 rad is measured in the $e_2$ direction, leading to a total phase shift of 20.40 ± 0.29 rad. The phase shift in the $e_2$ direction is much less than that in the $e_1$ direction, which tells us that the phase shift in the $e_2$ direction is due to the diagonal core pairs. In other words, the elongation in cores 1 and 2 (or 3 and 4) are the same since the inner/outer core pairs have the same bend radii, and they are expected to be stretched at the same rate. Measured phase shifts in the $e_1$ and $e_2$ directions together with the corresponding shear strains are summarized in the Table. The path-length difference $\Delta l$ is determined from Eq. (5) to be 1.66 $\mu$m and 0.71 $\mu$m for core pairs 1-3 plus 2-4 and 1-4 plus 2-3, respectively.

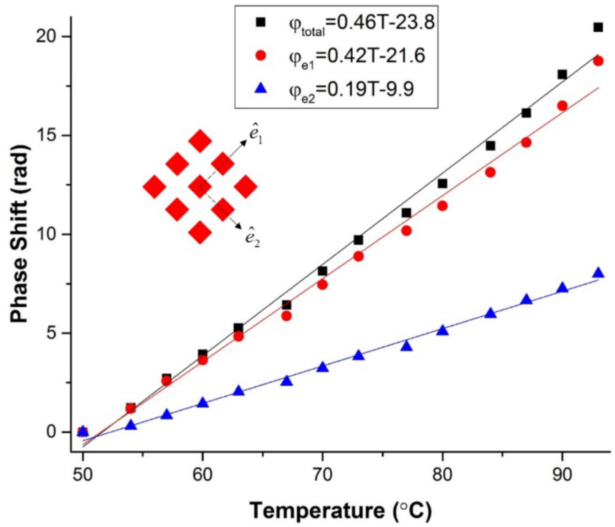


**Figure 5.** Phase change versus temperature in the $e_1$ and $e_2$ directions together with the total phase shift for a wound four-core fiber loop around a stainless steel solid cylinder.

**Table.** Phase shift and strain values in the $e_1$ and $e_2$ directions.

| | $e_1$ direction | $e_2$ direction |
|---|---|---|
| Phase shift (rad) | 18.76 | 8.01 |
| $\Delta l$ ($\mu$m) | 1.66 | 0.71 |
| $\varepsilon_{xx}$ (microstrain) | 13.50 | 5.77 |
| $\varepsilon_{xy}$ (millistrain) | 40.89 | 12.36 |

The temperature-induced phase and strain sensitivities of the four-core fiber are determined to be $\Delta\varphi/l\Delta T = 3.74$ rad/m°C and 0.18 $\mu\varepsilon$/°C, respectively. The temperature resolution of the device is determined to be 0.49 rad/°C, which is limited by the resolution of the CMOS camera (Optronis CR600x2). The camera could measure 15 mrad phase shifts, corresponding to 50 m°C degree changes.

In this experiment, power fluctuations have no effects on the determination of the phase shifting of the fringes and hence the resultant temperature-induced strain data. No power variations are detected in the system throughout the experiments. Even if there is a slight power variation in the optical system, this could only affect the fringe visibility slightly but not the phase measurement.

The transduction mechanism proposed here in this work has the potential to be a candidate for the construction of new fiber optic temperature sensors. Although the experiments are performed in the temperature interval between 50 °C and 92 °C, since the optical fiber's melting point is around 1100 °C [14], it is envisaged that the system can easily operate at temperatures beyond 92 °C unless the strain due to the thermal expansion of the rod causes any damage to the optical fiber material and its polymer jacket. For higher temperature operations, the strain experienced by the optical fiber may also be calculated with the expansion properties of the metal rod before the experiment. The tightness of the circular fiber loop around the stainless steel cylinder should be adjusted in such a way that the tensile strength of the fiber is able to withstand much higher temperatures so that the fiber does not break down.

As stated above, a straight piece of a four-core optical fiber is totally immune to external temperature variations since there are no cavities or internal/external mirrors associated to the fiber itself to give rise to any optical imbalance between the fiber cores. Our main contribution here in this work is to scheme out a new temperature-sensing transduction mechanism, which is based on strain-caused optical imbalance in the guiding cores of a four-core fused silica optical fiber.

The main advantage of this method is the flexibility to design a more sensitive device for a desired temperature range. Apart from the stainless steel rod, various types of materials can be employed in the experiment to induce different amounts of strain in the optical fiber. More sensitive sensors can be devised using materials with higher thermal expansion coefficient properties. In other words, one may consider a cylindrical material with high thermal expansion coefficient if the device is desired to be very sensitive. Similarly, a low thermal expansion coefficient material may be used to make use of the four-core fiber to achieve a much higher dynamical range, say up to the melting point of the polymer jacket, which covers the fused silica fiber, i.e. around 300 $^\circ$C. The dynamic range would have been directly proportional to the limit of the tensile strength and the melting point of the fused silica material, i.e. 1100 $^\circ$C, if it were possible to bend a bare fiber with the radii we used in our experiments. Unfortunately, one cannot form a circular loop with a bare optical fiber of more than 20–30 cm in diameter due to the brittle nature of fused silica glass. Another benefit of our scheme is that instead of using a known material as a thermally expanding rod, the thermal expansion of unknown materials can also be measured with the phase shift by the same experimental arrangement if one calibrates the system with a known cylindrical material first.

The experiment is repeated with several different rod diameters and the measurements are carried out several times for each sample. The results are observed to be repeatable. It is observed that larger diameters give higher sensitivity since the exposed fiber length is larger. The whole purpose of this work is to demonstrate the sensing mechanism, which is based on the strain-induced optical path-length difference between the fiber core pairs. If one aims to make use of this mechanism to build a temperature sensor, it would simply require calibrating the sensor with the rod diameter in concern. For a more compact sensor, a thin rod with several fiber loops would significantly enhance the sensitivity of the sensor.

To obtain reliable experimental results, the system must be well isolated from the external disturbing factors and the fringe pattern must be kept stable throughout the measurements. Since the optical fiber is sensitive to mechanical fluctuations and bending effects, the external parameters are eliminated by stretching and fixing both fiber ends using clamps as shown in Figure 3. The optical fiber must be kept tense at every point in the experimental setup to achieve a pure strain in the fiber cores. Although the four-core optical fiber used in the experiment provides a good interferometric fringe pattern, a small core spacing of 40.6 $\mu$m and large core diameters of 10.6 $\mu$m result in higher-order guided modes in the interferogram, causing an insignificant fringe stability problem since the four-core fiber was originally designed at the optical communication wavelengths. To overcome this problem, a four-core optical fiber with smaller core diameters and smaller core spacing should be used to obtain more stable and much clearer interference fringes.

Finally, one needs to make sure whether the curved fiber that is wound around the cylindrical rod has a twist within the curved region. In that case, a specific core would be compressed at some places and stretched at other places. This results in some sudden phase jumps in the phase of the guided light and hence sudden shifts would occur in the far-field interference pattern as the twist rescues itself. To overcome this problem, white light is coupled into the fiber cores to clearly observe each core under an optical microscope. The curved region is scanned under the microscope to avoid any fiber twist within the curved region around the cylindrical rod.

### 5. Conclusion

In this paper, the intrinsic and interferometric properties of a four-core fused silica optical fiber are utilized to demonstrate a novel temperature-sensing mechanism based on strain-induced optical path-length difference in the four guiding cores. An interferometric fringe pattern is obtained by the coherent waveguides from the four cores. A few centimeters of four-core fiber is wound very tightly around a stainless steel cylinder. The metal cylinder is exposed to a temperature rise to thermally expand, which leads to a shear strain in the fiber cores. Thus, the shift in the phase occurs from the optical path difference between the inner and outer core pairs. The amount of the strain is calculated through the measured phase data.

**Acknowledgment**

This project was supported by the Boğaziçi University Research Fund under contract number 10522.

## References

[1] Gholamzadeh, B.; Nabovati, H. *World Acad. Sci. Eng. Technol.* **2008**, *2*, 6.

[2] Lee B. H.; Kim Y. H.; Park K. S.; Eom J. B.; Kim M. J.; Rho B. S.; Choi H. Y. *Sensors* **2012**, *12*, 2467-2486.

[3] Gander, M. J.; Macrae, D.; Galliot, E. A. C.; McBride, R.; Jones, J. D. C.; Blanchard, P. M.; Burnett, J. G.; Greenaway, A. H.; Inci, M. N. *Opt. Commun.* **2000**, *182*, 115-121.

[4] Qu, H.; Yan, G. F.; Skorobogatiy, M. *Opt. Lett.* **2014**, *39*, 4835-4838.

[5] Yuan, L.; Wang, X. *Sensor Actuat. A-Phys.* **2007**, *138*, 9-15.

[6] Romaniuk, R.; Dorosz, J. *Proceedings of SPIE* **2012**, *4887*, 55-66.

[7] Antonio-Lopez, J. E.; Eznaveh, Z. S.; LiKamWa, P.; Schülzgen, A.; Amezcua-Correa, R. *Opt. Lett.* **2014**, *39*, 4309-4312.

[8] Aref, S. H.; Amezcua-Correa, R.; Carvalho, J. P.; Frazão, O.; Caldas, P.; Santos, J. L.; Araújo, F. M.; Latifi H.; Farahi F.; Ferreira L. A. et al. *Opt. Express* **2009**, *17*, 18669-18675.

[9] Bulut, K.; Inci, M. N. *Opt. Laser Technol.* **2005**, *37*, 463.

[10] Güvenç, S.; Gökbulut, B.; Kösoğlu, G.; Yüksel, H.; Inci, M. N. *Appl. Opt.* **2016**, *32*, 9173-9177.

[11] Blanchard, P. M.; Burnett, J. G.; Erry, G. R. G.; Greenaway, A. H.; Harrison, P.; Mangan, B.; Knight, J. C.; Russell, P. S.; Gander, M. J.; McBride, R. et al. *Smart Mater. Struct.* **2000**, *9*, 132-140.

[12] Burnett, J. G.; Erry, G. R. G.; Dickson, R.; McBride, R.; Gander, M.; Jones, J. D. C.; Blanchard, P. M.; Harvey, A. R.; Greenaway, A. H. In *Proceedings of the Applied Optics Divisional Conference*, 1998, pp. 105-110.

[13] Yılmaz, S. T.; Özuğurel, U. D.; Bulut, K.; Inci, M. N. *Opt. Commun.* **2005**, *249*, 515-522.

[14] Wallenberger, F. T. *Mater. Technol. Series* **1999**, 129-168.